Sensors and Actuators A 202 (2013) 140–146

Contents lists available at ScienceDirect

Sensors and Actuators A: Physical

journal homepage: www.elsevier.com/locate/sna

Ambient temperature and bias conditions induced frequency drifts in an uncompensated SOI piezoresistive resonator

C. Tu [a,b,*], J.E.-Y. Lee [a,b]

[a] Department of Electronic Engineering, City University of Hong Kong, Kowloon, Hong Kong
[b] State Key Laboratory of Millimeter Waves, City University of Hong Kong, Hong Kong

ARTICLE INFO

Article history:
Received 29 September 2012
Received in revised form 18 February 2013
Accepted 18 February 2013
Available online 6 March 2013

Keywords:
Piezoresistive sensing
Resonant frequency drift
Dog-bone resonator

ABSTRACT

Piezoresistive sensing has been demonstrated in literature to be more insensitive to geometric scaling and capable of affording substantially higher electromechanical conversion over capacitive sensing. Nonetheless, the bias current through the device required of this sensing method could lead to Joule heating effect and potentially introduce instabilities in the frequency. As such, the dependence of the resonance frequency on ambient temperature and bias conditions in such case becomes more complicated and needs to be examined. In this paper, we track the resonant frequency of such a piezoresistive resonator together with the ambient temperature over 15–25 h. We have found that the frequency shifts can be correlated with changes in ambient temperature. Additional frequency drifts due to the bias current were not observable even when the bias current was as high as 5 mA (corresponding to 4 mW of power), which was enough to yield a resonant peak of 24 dB above the capacitive feedthrough floor. Also, it was experimentally observed that the resonant frequency is dependent on the bias current or voltage.

1. Introduction

Nano and micro mechanical resonators have been extensively investigated for mass sensing applications [1], which can afford high mass sensitivity due to their small form factors. By using a length-extensional bulk mode resonator with annexed platform, Hao et al. have demonstrated a mass sensor with a mass sensitivity of 215 Hz/pg with an accompanying *Q* of 4000 in air [2]. Another mass sensor based on a square-extensional mode resonator was subsequently proposed [3], which achieves a mass sensitivity of 3.3 Hz/ng and *Q* exceeding 10^6 at an operating pressure of 3.8 mTorr. As typified by these two examples of resonant sensors, a combination of capacitive drive and sense is commonly used in fully electrically interfaced resonators. The main challenge with capacitive sensing is that as form factors are reduced to increase mass sensitivity, transduction is also reduced. This in turn leads to larger motional impedances [4].

In comparison to capacitive sensing, van Beek's analysis [5] has previously shown that a micromechanical resonator employing piezoresistive sensing could be insensitive to geometric miniaturization. Piezoresistive sensing in addition generally affords higher electromechanical transduction compared to capacitive sensing. One of the examples is the recent demonstration of a piezoresistive MEMS oscillator operating in air [6]. More recently, by using a dog-bone resonator that employs piezoresistive sensing, we have demonstrated a reduction in the insertion loss by over 500 times compared to capacitive sensing [7]. Another intriguing property of micromechanical resonators employing piezoresistive sensing is that they have the potential to achieve self-sustained oscillation, without the addition of amplifying electronics [8]. By using piezoresistive sensing so as to provide better impedance matching, Li et al. was able to implement an ultra-sensitive nanoelectromechanical mass sensor that could even detect the Brownian noise vibrations in air [9]. In addition, since the piezoresistive property is inherent to silicon, as shown previously by Lin et al. [10], the piezoresistive transducers could come as part of the lithographically defined structure. As such, no additional fabrication steps are required.

Though piezoresistive sensing has numerous advantages over conventional capacitive sensing as briefly highlighted above, one of the concerns involves Joule heating in the device as well as noise associated with the bias current running through the resonator as required in piezoresistive sensing [11,12]. The Joule heating effect could potentially introduce noise and instabilities in the resonant frequency of the resonator, which could greatly compromise the mass sensitivity of the mass sensor as well as the stability of the reference frequency if used as an integrated MEMS oscillator. On this note, we have previously shown that running a moderate level of current (0.82 mA) through the resonator produces no observable effect on the frequency drift of the device [12]. It was found that the observed drift in resonant frequency measured over almost a

* Corresponding author at: Department of Electronic Engineering, City University of Hong Kong, Kowloon, Hong Kong. Tel.: +852 34422656; fax: +852 34420562.
E-mail addresses: mems305@gmail.com (C. Tu), joshua.lee@cityu.edu.hk (J.E.-Y. Lee).

0924-4247/$ – see front matter
http://dx.doi.org/10.1016/j.sna.2013.02.023

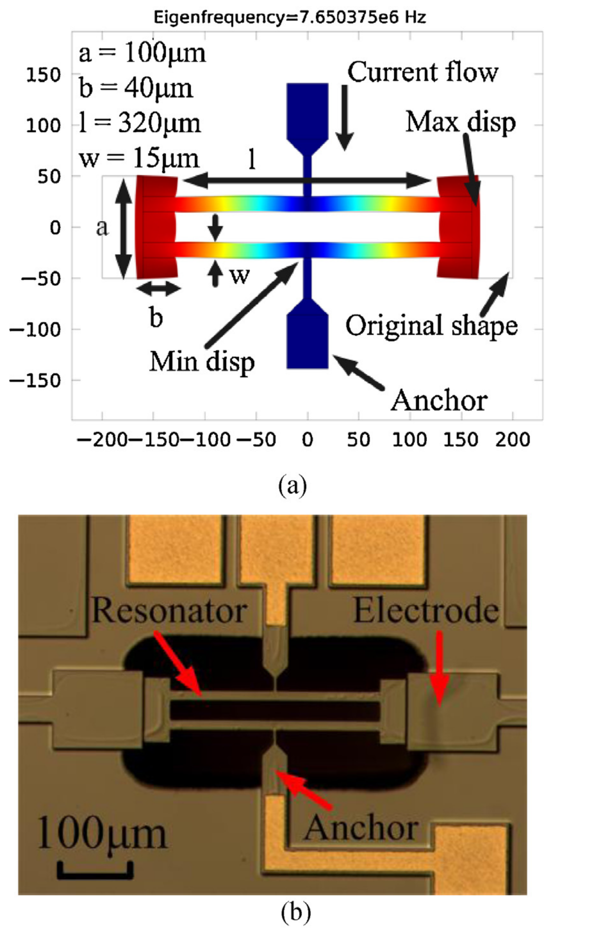

Fig. 1. (a) FE simulation of the length-extensional mode in the dog-bone resonator using COMSOL. "Min disp" and "Max disp" denote minimum and maximum displacements respectively. (b) Optical micrograph of the fabricated SOI dog-bone resonator.

full day could well be accounted for by just the temperature coefficient of frequency of the resonator. The current was applied then through a controllable current source. In this work, we consider the resultant resonant frequency drifts at higher currents (up to 5 mA) which are applied through a controllable voltage source.

The next section provides a description of the resonator and its working principle that allows piezoresistive sensing. Section 3 presents the measurements of the frequency tracked over time simultaneously with temperature. In Section 4, the implications of these results are discussed.

2. Design and simulation

The device investigated in this work is described in Fig. 1(a), which shows a finite element (FE) simulation of the vibration mode shape. It can be seen that the resonator comprises a parallel pair of beams which are terminated on each side by a proof mass. The geometry of the resonator is similar to that presented in [5], with the addition of extra proof mass. Each of the beams is anchored midway along their lengths. As shown in Fig. 1(a), the beams expand and contract longitudinally, with minimum extension at the center and maximal extension at the ends. We refer to this topology in this paper as a dog-bone resonator. Referring to Fig. 1(b), which provides an optical micrograph of the device, it can be seen that anchored electrodes are fabricated on each side of the dog-bone resonator. The proof mass and electrodes form a capacitive gap transducer that is used to excite the resonator into the desired mode

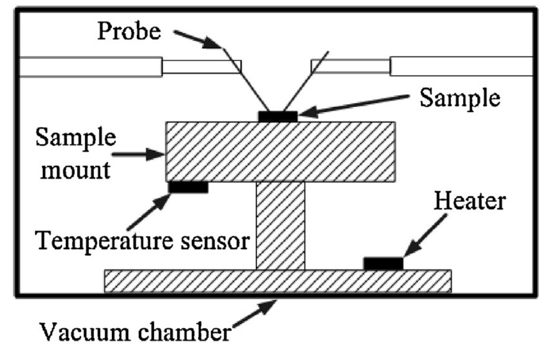

Fig. 2. Measurement setup in the vacuum chamber of the probe station.

of resonance by electrostatic actuation. By anchoring the beams at their center where the reaction forces from both tines balance, loading of the anchors is minimized, thus leading to high quality factor (Q). It may be seen that as the beams expand and contract, the axial stress in the beams allows them to be used as piezoresistors owing to the inherent piezoresistive property in silicon. Hence by dropping a voltage across the anchors, a modulated motional current results from the change in resistance.

The resonant frequency of the dog-bone resonator is given by [13]

$$\frac{\omega l}{2v}\tan\left(\frac{\omega l}{2v}\right)=\frac{M_b}{M_p} \quad (1)$$

where ω is the angular resonant frequency, l denotes the length of the central beam, v is the velocity of the longitudinal wave, M_b and M_p represent the mass of the beam and proof mass respectively. The resonant frequency calculated from Eq. (1) is 7.773 MHz, which is 1.6% higher than the simulated prediction. This small difference is expected since Eq. (1) assumes that the beams undergo only contraction or expansion along the longitudinal direction along the length, while the FE simulations shows that the beams in fact flex slightly as they expand and contract longitudinally. The resonator has been fabricated in a standard silicon-on-insulator surface micromachining process with a capacitive gap of 2 μm and a device thickness of 25 μm.

The dog-bone resonator makes a suitable choice for mass sensing applications since the proof mass on both ends approximate to rigid bodies relative to the beams, as can be seen from the FE simulation. As such, particle absorption on the two heads has little effect on the equivalent stiffness and mass loading becomes the dominant mechanism for perturbing the resonant frequency. Such compact structures typically come with the tradeoff of reduced electromechanical coupling. However, this could be addressed by using piezoresistive sensing to provide better electromechanical coupling [5] as will be shown in Section 3. However, as piezoresistive sensing requires a current through the device, this could result in introducing noise into the electrical transmission that could potentially affect the frequency stability of the device. This issued is studied in the next section which presents measurements of the electrical transmission tracked over at least 15 h.

3. Measurements

3.1. Bias current applied by fixing DC voltage

The device was measured under vacuum in a cryogenic probe station thus reducing as far as possible the effect of moisture on frequency drift. Fig. 2 shows the measurement setup. The temperature sensor is located in the sample mount (that also functions as a heat chuck) on which the sample die is placed. As such, all